Full Paper Transactions, SMiRT 28
Toronto, Canada, August 10-15, 2025

SEISMIC SSI ANALYSIS INVESTIGATIONS FOR EFFICIENT DESIGN OF BASE-ISOLATED DEEPLY EMBEDDED ARC-100 SMR

Dan M. Ghiocel [1], Daniel Lemley[2], Jeff Pieper[3] and Enver Odar[4]

[1] Ghiocel Predictive Technologies, Rochester, New York, USA (dan.ghiocel@ghiocel-tech.com)
[2] United Engineers & Constructors, Mt Laurel, New Jersey, USA
[3] Hopper Engineering Associates, Walnut Creek, California, USA
[4] ARC Clean Technology, Washington, D.C., USA

ABSTRACT

The paper addresses key seismic soil-structure interaction (SSI) modelling and analysis aspects related to the base-isolated deeply embedded ARC-100 SMR structure using Friction-Pendulum (FP) bearings placed at a single moat upper baseslab well below the ground surface level. The paper is a continuation of a previous SMiRT27 research paper (Ghiocel et al., 2024). This paper addresses key seismic SSI modelling aspects for the deeply embedded base-isolated SMR focusing on the effects of the potential subsystem dynamic coupling between the superstructure and reactor vessel (RV) system responses, and the input random variations and modelling uncertainties on the isolated structure response. The investigated input random variations include DBE seismic motion spectral amplitude variations, FP isolator system stiffness variations including stiffness space variations producing mass eccentricities, variations due to single FP isolator failure at different locations, and variations of due to seismic wave nonsynchronous propagation (including incoherency and wave passage effects). The paper also discusses how to improve the SMR base-isolation system efficiency using a *hybrid* isolation system by integrating the *global* isolation system using the 2D FP bearings with a *local* isolation system using the 3D Base Control System (GERB BCS) devices including a combination of 3D springs and 3D viscous dampers placed at the RV top supports. The seismic SSI analysis results indicate that a hybrid isolation system appears highly desirable for avoiding potential dynamic coupling between the SMR superstructure and RV system. Currently, a base-isolation solution is investigated using *a global* 3D BCS isolation instead of a *global* 2D FP isolation.

ARC-100 SMR CASE STUDY

The objective of this paper is to provide key technical insights on the seismic SSI analysis of the base-isolated deeply embedded ARC-100 SMR structure design. The SMR embedment depth is 66.5 ft. The investigated base-isolation system solution was a 2D global isolation system made by a set of 28 Friction Pendulum (FP) hysteretic isolators distributed at the SMR upper foundation base-level at a 43.5 ft depth below ground surface as shown in Figure 1. The basis of this paper is a multiyear advanced conceptual study focused on establishing the design-basis seismic SSI analysis methodology of the base-isolated embedded ARC-100 SMR structure, but at the same time identifying and quantifying the effects of some key influential factors, such as random input variations or modelling assumptions, which potentially could affect the final ARC-100 SMR design-basis analysis procedure.

It should be noted that up to this date, there is no accumulated nuclear industry design experience for deeply embedded seismically base-isolated SMR designs. The base-isolated ARC-100 SMR innovative design is also a test on the applicability and practicality of the recent ASCE 4-16, ASCE 43-19 and ASCE 7-22 standard recommendations for performing the seismic SSI analyses for base-isolated deeply embedded SMR structures. So far, the ASCE standards focus has been on base-isolated surface structures.

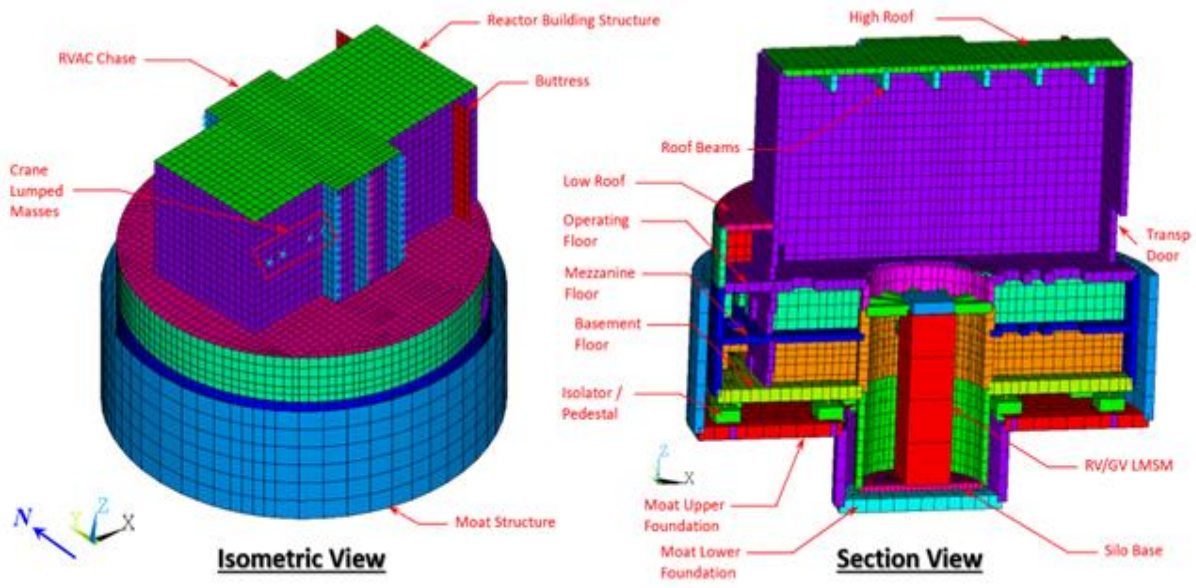

Figure 1 Seismically Base-Isolated ARC-100 SMR Structure Model

The two-step seismic SSI methodology described in Figure 2 was explained in relative detail in a previous paper (Ghiocel et al., 2024). *Step 1* performs an iterative seismic linearized SSI analysis, based on a hybrid complex frequency domain-time domain approach using bilinear hysteretic models for FP isolators, to accurately determine the SSI foundation response motion for the equivalent-linear FP isolator properties. *Step 2* performs a nonlinear dynamic analysis of the isolated superstructure, based on a time-domain approach using highly refined nonlinear FP isolator models (Fentz and Constantino, 2008) excited by the SSI response motions computed at the isolator pedestal support locations.

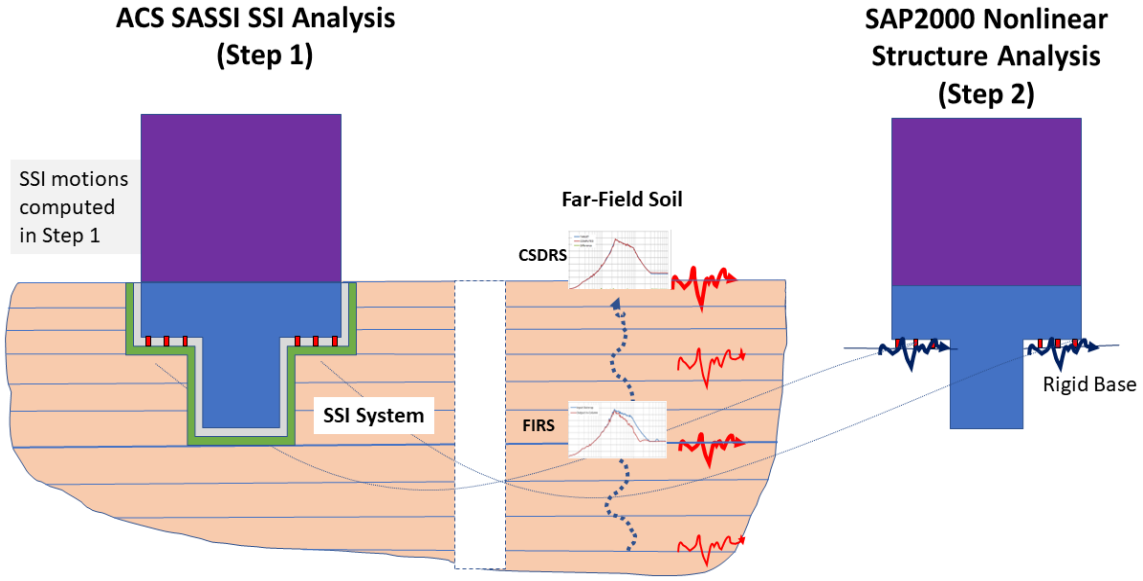

Figure 2 Two-Step Seismic SSI Analysis Applied to Deeply Embedded Base-Isolated ARC-100 SMR

The ACS SASSI Option NON software was used for Step 1, and the SAP2000 software was used for Step 2. SAP2000 includes a detailed FP bearing nonlinear modelling in time-domain.

The 28 FP isolator distribution was on two circular line locations are shown in Figure 3 (left). All isolators were of the FPI 15680-26 type (see https://www.earthquakeprotection.com/) with different gravity axial forces from 1373 kips to 3371 kips as shown in Figure 3 (right).

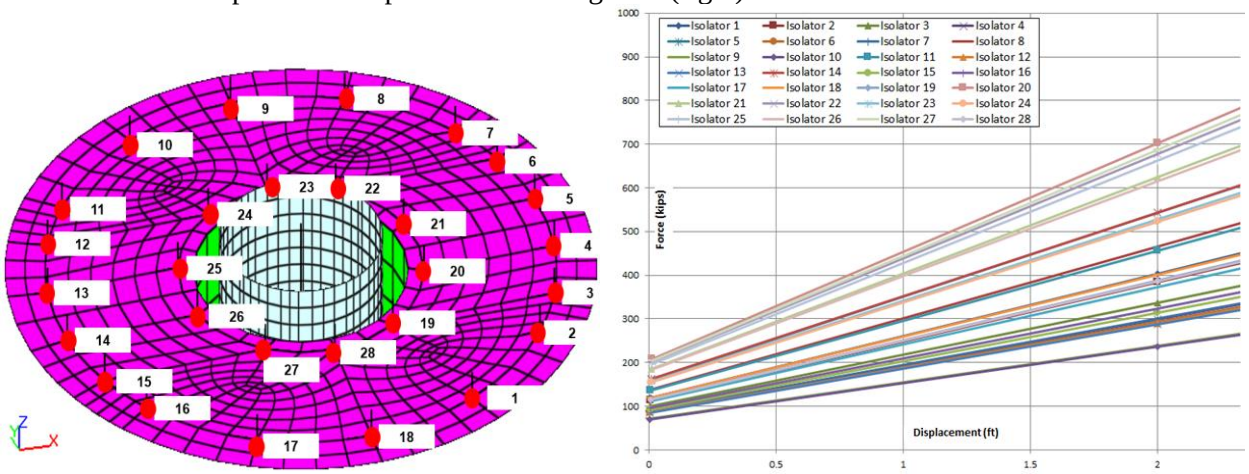

Figure 3 The FP Isolation System; FP Isolator Locations (left) and Back-Bone Curves (right)

Two generic site conditions were considered in the study, specifically, a firm soil site condition (Vs=2,000 fps) and a hard-rock site condition (Vs=8,000 fps) as shown in Figure 4. The CSDRS shape for the firm soil site follows exactly the RG1.60 spectrum shape, while the CSDRS-HF (High-Frequency) shape for the hard-rock site follows closely the Seabrook site-specific spectrum shape. The soil site CSDRS is representative for Western US, while the rock site CSDRS-HF is representative for Central and Eastern US. The maximum acceleration at ground surface was considered 0.50g for both generic site conditions. The CSDRS inputs plotted in Figure 5 were applied to both horizontal and vertical directions.

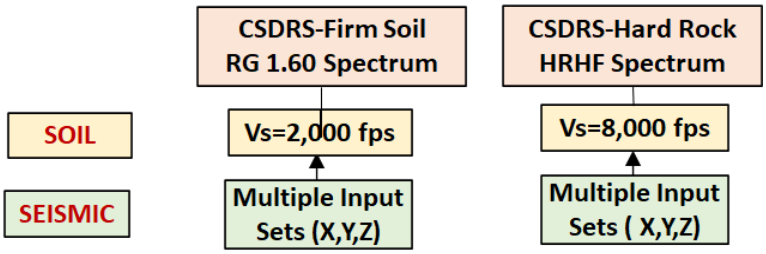

Figure 4 Selected Generic Site Conditions for this Study

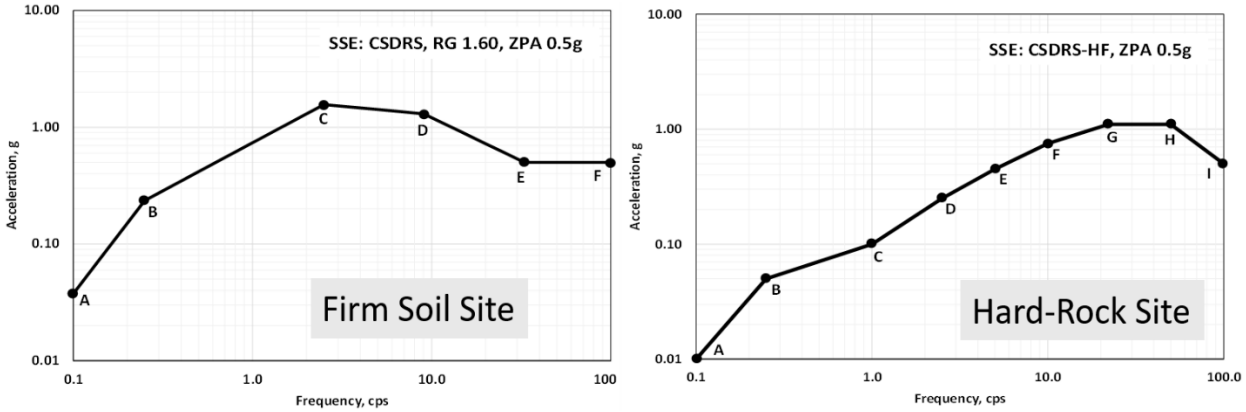

Figure 5 Firm Soil CSDRS and Hard-Rock High Frequency CSDRS-HF Inputs

It should be noted that to fully cover the entire frequency range of interest, additional soil sites should be considered for the standard plant design. However, it was agreed that for this Advanced Conceptual Design study, using only two very different generic site conditions are sufficient for demonstrating the seismic SSI design-basis methodology for the base-isolated deeply embedded ARC-100 SMR structure for both the firm soil type and the rock type of sites.

The SSSI effects were also considered by including all the SMR Reactor Building structure, Radwaste Building (RWB) structure and Control Building (CB) structure into a single SSSI model described in Figure 6. The SSSI effects were included only for the firm soil site.

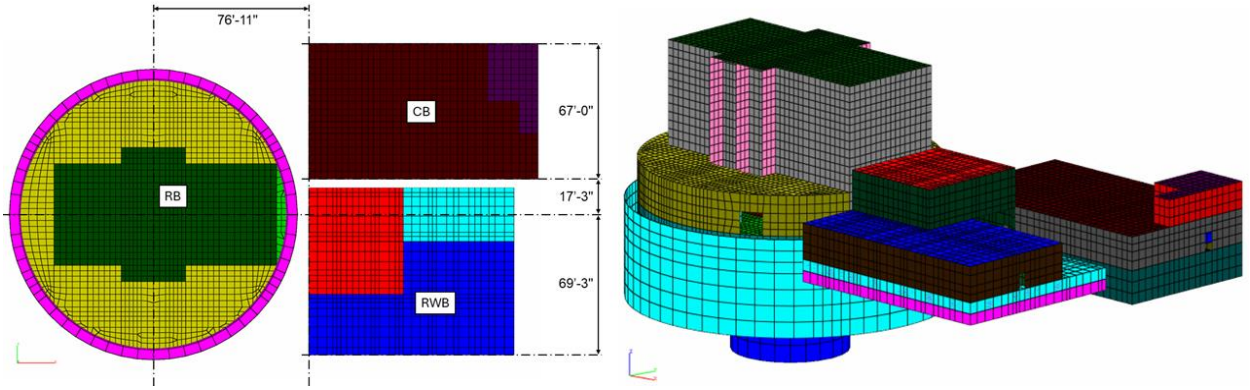

Figure 6 ACS SASSI Seismic SMR-CB-RWB SSSI Model Used for Soil Site

ASCE STANDARD REQUIREMENTS FOR BASE-ISOLATED STRUCTURES

The ASCE 4-16 Chapter 12 applicable to base-isolated structures requires for the DBE shaking to compute the mean and 80th percentile seismic responses. To be compliant with the most updated requirements, including the new ASCE 7-22 standard requirements to compute the 80th percentile DBE responses, 11 seismic input sets combined with 3 soil variations, specifically the lower-bound (LB), the best-estimate (BE) and upper-bound (UB) soils, were considered for each generic site condition. In accordance with the ASCE 4-16 Section 5.1.7, the 0.50 coefficient of variation of the soil shear modulus is the minimum variation acceptable for a deterministic SSI analysis for well-investigated soil sites. Therefore, for the DBE shaking and for each of the two generic site conditions, 33 seismic SSI analysis simulations were considered (33 = 11 input sets x 3 soil variations, BE, LB and UB soils). The mean and 80th percentile maximum DBE responses were determined based on the 33 SSI analysis simulations for each generic site condition.

For each soil variation (LB, BE and UB soils), 11 spectrum compatible seismic input sets were required. For the two CSDRS types, a total of 22 input sets of spectrum compatible acceleration triplets for the X, Y and Z directions were generated. Therefore, a total of 66 acceleration time histories (66 = 2 CSDRS type x 11 sets x 3 components) were generated for the DBE shaking. Each generated acceleration had a maximum ground acceleration of 0.50g. The 22 sets of seismic input acceleration triplets were generated in accordance with the NRC SRP 3.7.1 Rev 4 requirements for the Option 2 (multiple sets of time histories), which is applicable to multiple input sets of acceleration time histories, but at the same time is in compliance with the more restrictive Option 1 (single set of time histories) Approach 2 which is applicable to each generated acceleration time history.

The CSDRS compatible acceleration time histories were generated using the ACS SASSI EQUAKE module which includes a refined acceleration baseline correction algorithm for accurate computation of the velocity and displacement time histories, and provides detailed information on the various parameters of the generated motion, including the peak acceleration, velocity, and displacement, as well as the PSD of the strong motion interval defined for the Arias intensity variation from 5% to 75%. The statistical correlation coefficients between the three motion components were also checked.

Following the NRC RIL 2019-01 (Nie, 2019) recommendations for Option 1, Approach 2, the strong motion interval PSD of generated accelerations were checked per NRC SRP 3.7.1 Appendices A and B to ensure that there is no frequency content deficiency for the generated time histories, especially for the low-frequency content. The computed simulated and average PSD for the 11 generated accelerations for the firm soil site and, respectively the hard-rock site, are shown in Figure 7.

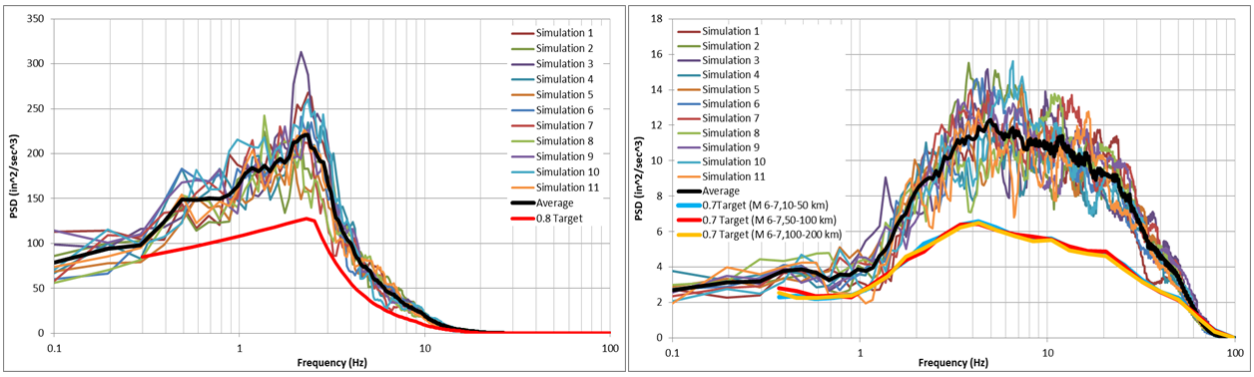

Figure 7 The 11 Simulated and Average PSD vs. Minimum Target PSD for CSDRS Input for Soil Site (left) and CSDRS-HF Input for Hard-Rock Site (right).

FP BASE-ISOLATED EMBEDDED ARC-100 SMR STRUCTURE SEISMIC SSI REPONSES

Figure 8 shows the SSI relative displacements of the isolated SMR structure for the FP isolator # 12 with respect to the foundation input motion for the 11 seismic input sets of spectrum compatible acceleration triplets associated with the BE soil profiles for the firm soil site and the hard rock site, respectively. It should be noted that for the BE soil and CSDRS input, the isolator displacements are up 1.7 ft, while for the BE rock and CSDRS-HF input, the isolator displacements are up to only 0.05 ft. This indicated a reduction in the FP isolator sliding displacement of about 35 times for the rock site versus the soil site. The main driver of this large reduction of the isolator displacements is the seismic input frequency content which largely impacts on the ground motion displacements. The large reduction of the isolator displacements for the rock site is also due to the fast sign-switching acceleration motion for the CSDRS-HF high-frequency motion.

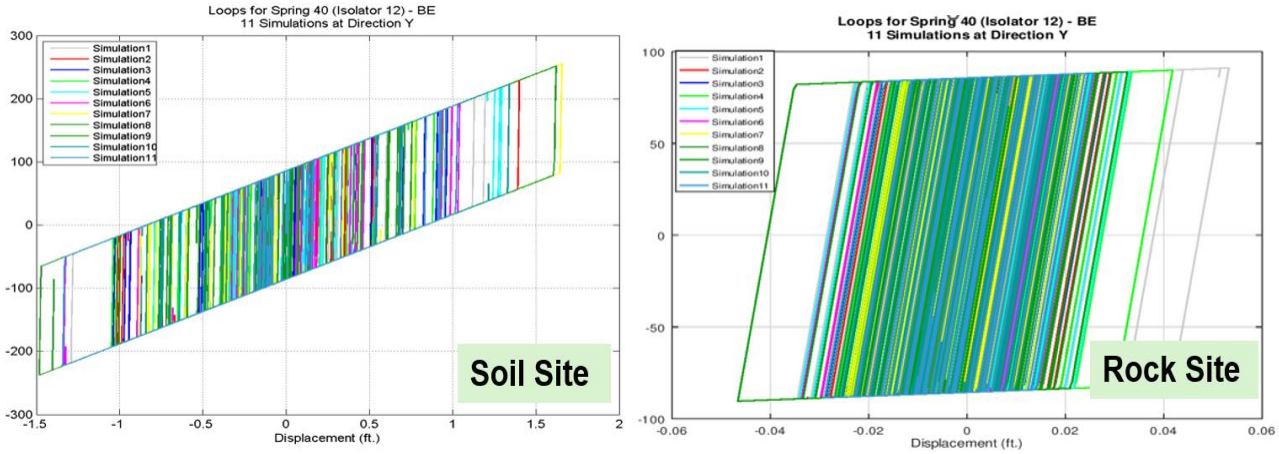

Figure 7 FP Isolator #12 Seismic Sliding Displacements for Firm Soil (left) and Hard-Rock (right)

Figures 8 and 9 show the mean and 80th percentile ISRS in the X and Y directions (including also the 33 sample ISRS) for the soil site and rock site at a roof top corner of the SMR structure (Node 6390) at

Elevation 64.75 ft. The maximum SSI response SMR roof accelerations are quite low for isolated structure, being only 0.20-0.25g for soil and 0.25-0.35g for rock, well below the 0.50g ground surface acceleration.

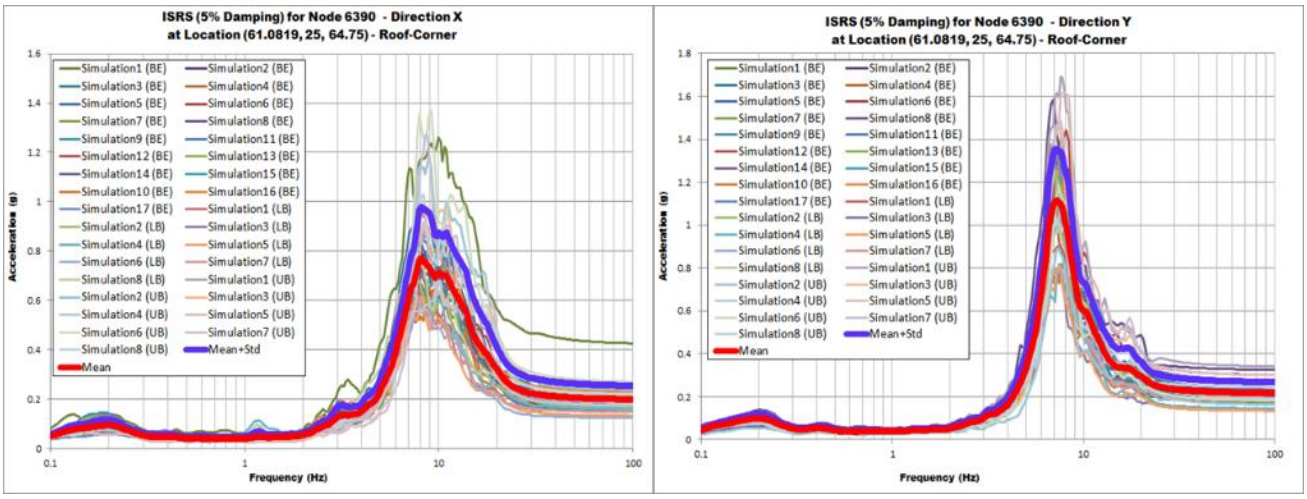

Figure 8 33 Simulated, Mean and 80th Percentile ISRS at SMR Roof Corner (El. 64.75 ft) for Soil Site

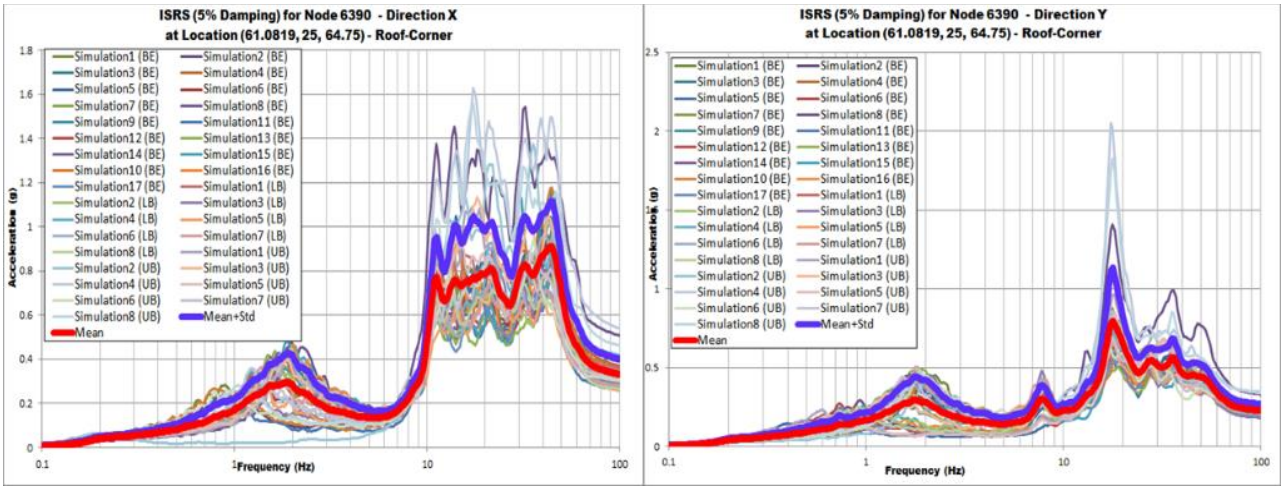

Figure 9 33 Simulated, Mean and 80th Percentile ISRS at SMR Roof Corner (El. 64.75 ft) for Rock Site

Figure 10 shows the computed mean and 80th percentile ISRS for isolated SMR for the soil site and rock sites at two extreme elevations (upper plots), at -56.5ft at the RV stick bottom (Node 16239) and at 64.75ft at the roof (Node 7075), in comparison with the ground surface elevation (lower plots). The ISRS plots indicate high spectral amplifications for the two extreme elevations (at RV bottom and SMR roof) at around 8-9 Hz for the soil site and around 18 Hz for the rock site. The large spectral amplification at the same frequency appears to indicate a dynamic coupling between the isolated SMR structure response and RV stick bottom response.

The largest motion amplification is at the RV stick bottom end at around 8-9 Hz for the soil site in X direction. A more modest, but still visible motion amplification is also noted at the RV bottom end at around 18 Hz for the rock site. For the soil site in X direction the ISRS computed the RV stick bottom locaton has a mean spectral peak amplitude of 4.4g which is extremely high for the isolated SMR structure.

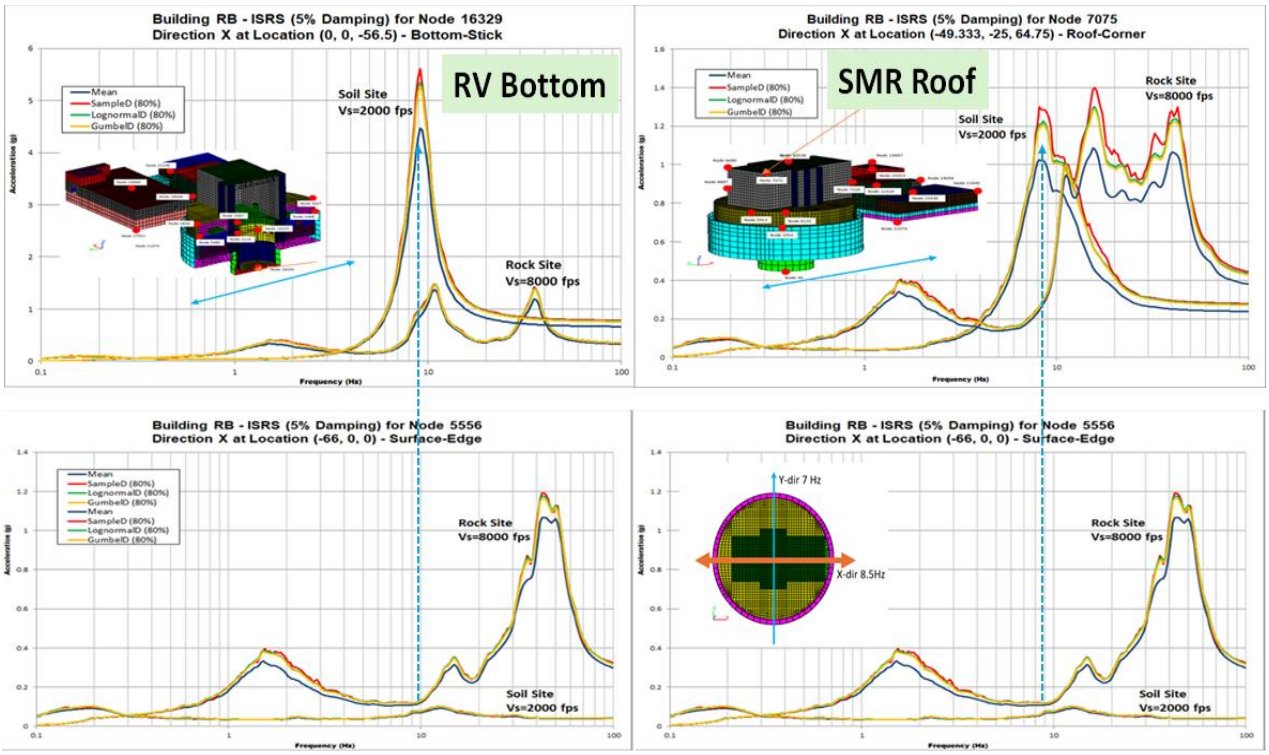

Figure 10 Mean and 80th Percentile X-Horizontal ISRS at RV Bottom (Node 16329) and SMR Top Corner (Node 7075) (upper plots) in Comparison with ISRS on SMR Wall at Ground Level (lower plots)

Figure 11 provides a much more intuitive visual explanation for the differences between the SMR structural acceleration responses in X and Y directions. The figure shows the SMR structural acceleration responses at an arbitrary instant time in the X and Y directions for the soil site.

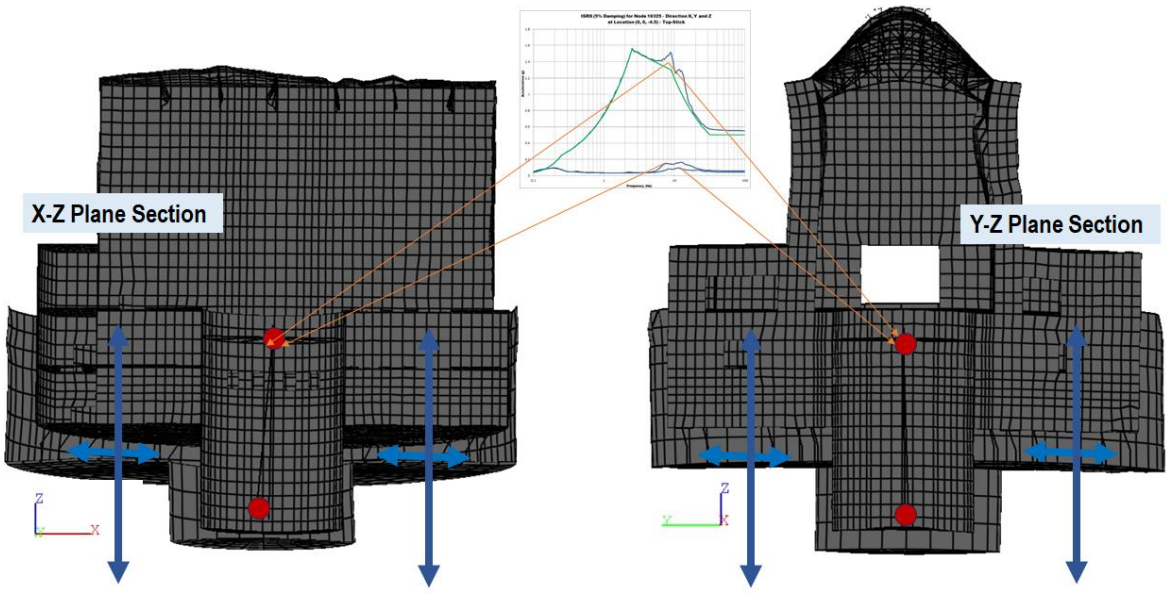

Figure 11 SMR Instant Accelerations for X-Direction (left) and Y-Direction (right) for Soil Site

The lack of perfect symmetry for the SMR structure in the X-Z plane produces a very small SSI rocking motion which for the soil site stiffness creates a certain condition for a large vibration energy transfer from

the vertical response to the horizontal response due to a multiple SSI mode frequency tuning. It should be noted that this dynamic coupling is not visible for the Y-direction responses which are apparently independent of the vertical motion response. This dynamic coupling in X-direction due to multiple mode frequency tuning is strictly related to the SSI effects for the soil site stiffness corresponding to a soil shear wave velocity of 2,000 fps. The dynamic mode coupling is also due to the limitation of the FP isolators that are efficient only for the horizontal responses but have no effect on the vertical responses which remain large with a large amount of vibration energy.

To add a quantitative checking measure for evaluating the dynamic coupling effects, we compared the ISRS computed at the RV stick bottom and at the top of SMR structure locations for the vertical input acceleration of 0.5 g and a 25% reduced vertical input acceleration, specifically 0.375g = 0.75 x 0.50g. Figure 12 shows these ISRS comparisons for the two locations. It should be noted that the horizontal ISRS peaks at the two locations in X-direction reduces by about 23%, while the ISRS peaks in Y-direction show only a very small reduction, basically, showing almost no coupling with the SMR vertical motion.

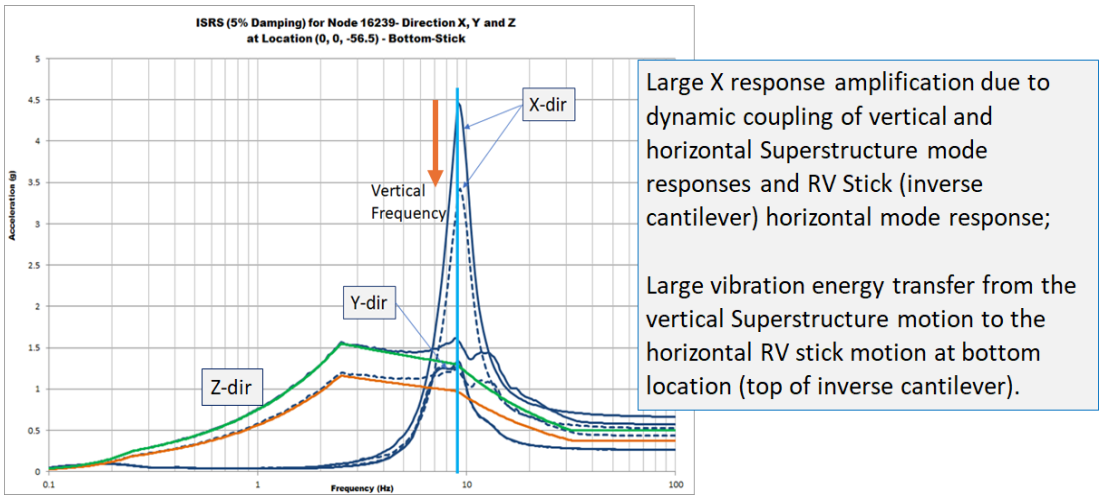

Figure 12 Horizontal and Vertical ISRS at RV Bottom Location (Node 16329) for the Soil Site for Vertical Acceleration Input of 0.50g (solid line) and 0.375g = 0.75 x 0.50g (dashed line)

Based on the above results, it was concluded that the high amplified response accelerations at the RV stick bottom in X direction (Node 16329) due to factors such as soil conditions, proximity of RV cantilever frequency of vibration to the frequency of vibration of the RB structure in X direction are resulting in a severe dynamic coupling which needs to be avoided.

Due to these unacceptably high seismic acceleration responses of the RV system which occurred for the soil site, some remedial actions were considered using a hybrid isolation system as explained in next section.

CONSIDERING A HYBRID ISOLATION SYSTEM TO IMPROVE RV SYSTEM RESPONSE

To reduce the large RV acceleration responses for the soil site, a local 3D isolation system was introduced at the RV stick beam supports. Therefore, a *hybrid* isolation system was created by integrating the *global* isolation system using the 2D FP bearings with a *local* isolation system using the 3D BCS devices (see https://www.gerb.com) which are combined 3D spring blocks (SB) and 3D high-viscosity dampers (HVD) placed at the 12 RV top beam supports as illustrated in Figure 13.

It should be noted that ACS SASSI NQA V4 software includes a specialized HVD finite element to model the frequency-dependent dynamic behaviour of the GERB 3D HVD units. Each HVD element incorporates two parallel 2-parameter Maxwell Chain models including a total eight input calibration parameters to be user defined based on test data.

Two BCS configurations were considered: 1) Model 1 including 12 SB and 6 HVD units, and 2) Model 2 including 12 SB and 12 HVD units as described in Figure 13.

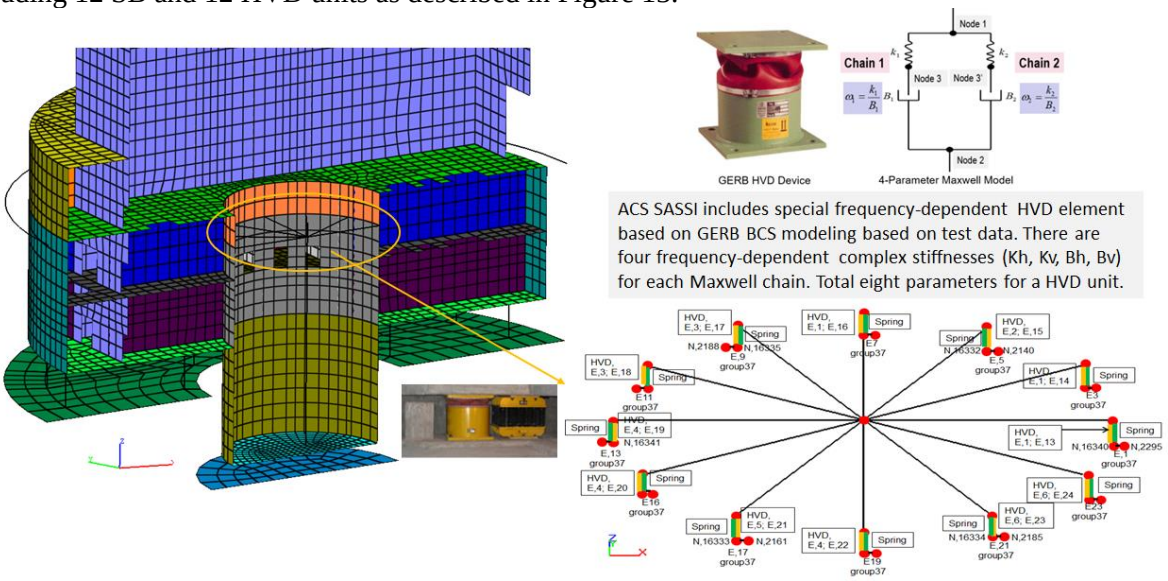

Figure 13 Local 3D BCS Isolation Model Placed at RV System Support Beams

The SSI results were compared for three models, including the original FP base-isolated SMR model with no BCS devices (Model 0) and the two hybrid FP base-isolated SMR models including BCS devices for the local RV system base-isolation. For the preliminary calculations, only a single seismic input set was considered.

Figure 14 shows the ISRS computed in X-direction for Models 0, 1 and 2 at the RV system top and bottom ends (Nodes 16325 and 16329). The computed ISRS show that introducing the 3D isolation devices at the RV beam supports (Models 1, 2) drastically reduces the RV system horizontal acceleration responses. Basically, the inclusion of the 3D BCS devices at the RV top supports completely avoids the system dynamic coupling described in the previous section, Figure 11.

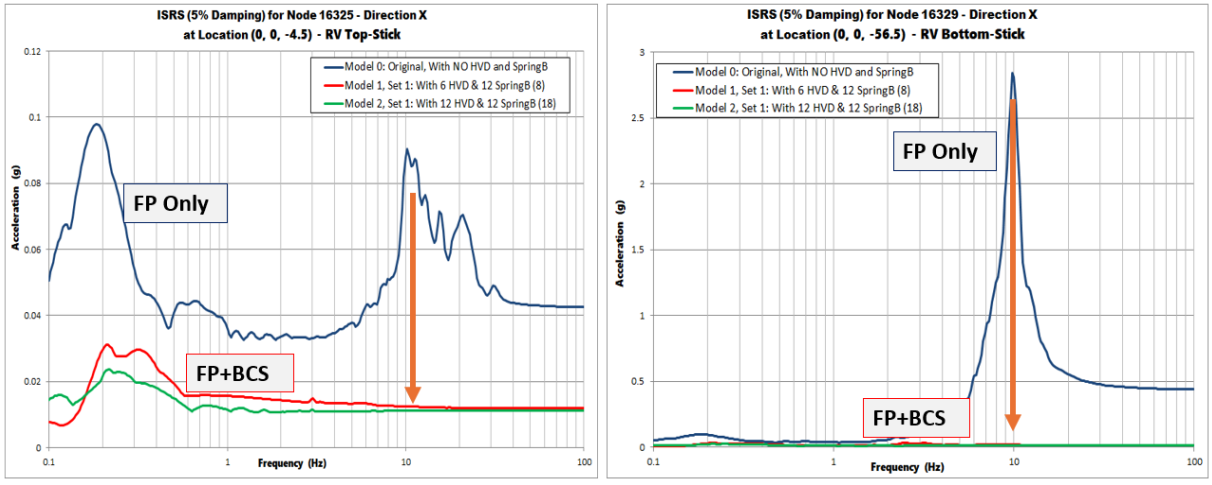

Figure 14 ISRS at RV System Top (Node 16325) and Bottom Ends for Soil Site in X-Direction

It should be noted that the ISRS computed at other locations within the isolated SMR structure in all directions showed only a very small difference, practically negligible, between computed ISRS for Models

0, 1 and 2. As expected, the ISRS in the vertical direction showed that the local BCS isolation devices placed at the RV supports do not bring any isolation improvement in the vertical direction.

SEISMIC SSI SENSIVITY INVESTIGATIONS FOR INPUT VARIATIONS

These preliminary SSI sensitivity studies were limited to some key influential effects due to

1. DBE spectral amplitude variations, including component-component variations
2. FP isolation system stiffness random variation
3. Mass eccentricity variations due to the FP isolation system stiffness spatial variation
4. Single FP isolator failure assuming scenarios for different locations
5. Seismic motion spatial variation due to presence of non-vertically propagating waves

From these preliminary SSI sensitivity studies, items 4 and 5, which appeared to have the largest influence on ISRS responses are discussed herein.

Effects of Single FP Isolator Failure

For the soil site the largest ISRS differences due to single isolator failures were below 10-15% at higher elevations. In contrast, for the rock site the largest ISRS differences due to the single isolator failure go up to above 100% in few locations at higher elevation levels, as shown in Figure 15. The high frequency SSI responses being dominated by local higher-order mode shapes are much more sensitive to the local changes in the FP isolator stiffness distribution due to the loss of an isolator.

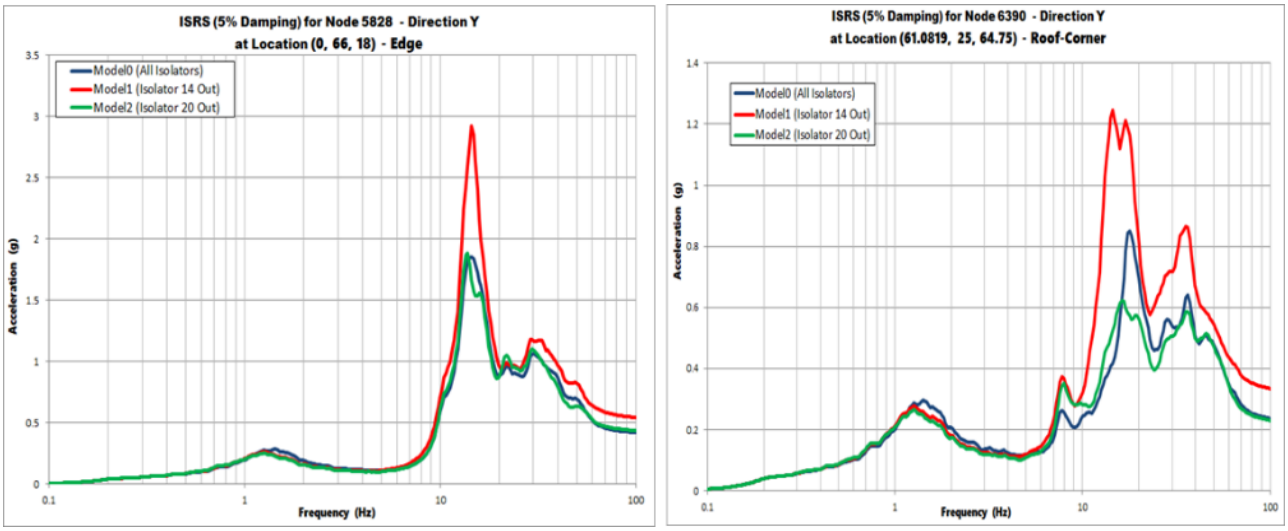

Figure 15 Comparative Horizontal ISRS at Two SMR High Elevations, at18 ft and 64.75 ft (Nodes 5828 and 6390) for Models 0, 1 and 2 for Rock Site

Effects of Seismic Motion Spatial Variation (due to Wave Incoherency and Wave Passage)

To study motion spatial variation effects, the seismic input was defined by 11 sets of triplets of spectrum compatible accelerations for CSDRS for soil site and CSDRS-HF for rock site, while the soil stiffness was defined by the BE soil profiles, V_s=2,000 fps for soil site and V_s=8,000 fps for the rock site. The incoherent input motions were defined for the two generic sites based on the Abrahamson models (Abrahamson, 2007) for the soil site and rock site. The wave passage effects were also included by defining an apparent wave velocity along an oblique 45 degrees direction with respect to the X and Y axes. The apparent wave velocity was taken as V_a = 5,000 fps for the soil site and V_a = 25,000 fps for the rock site.

The ACS SASSI NQA V4 Stochastic Simulation (SS) approach was applied. The incoherent SS approach uses a rigorous Monte Carlo simulation for generating the 11 sets of the seismic incoherent wavefield based on the Abrahamson stochastic coherency models.

The mean ISRS responses were computed for the 11 sets of coherent and incoherent simulations. Herein we show the ISRS comparisons at a low elevation of -16 ft (Node 2280) on the RV containment within the isolated SMR structure. The comparison is between the coherent mean ISRS (red line) and the incoherent mean ISRS (green line). The 11 incoherent ISRS samples are included with thinner coloured lines.

For the soil site, as shown in Figure 16 the horizontal motion spatial variation largely amplifies the mean ISRS responses in the 1.5-2.5 Hz frequency range. These large ISRS spectral amplifications are due to the incoherent wave differential soil motions that can randomly excite isolated structure rocking modes in this frequency range as shown for many samples. The ISRS spectral amplification is more pronounced in the X-direction which is sensitive to the increased vertical-horizontal coupling (as discussed in previous section) due to the differential support motions than in the Y-direction. These randomly excited rocking modes are not excited by the "deterministic" 1D coherent wave motions that include no free-field differential soil motions in horizontal plane due to the purely theoretical assumption of perfectly vertically propagating waves. As expected, the simulated incoherent ISRS random samples show a large statistical scatter from sample to sample.

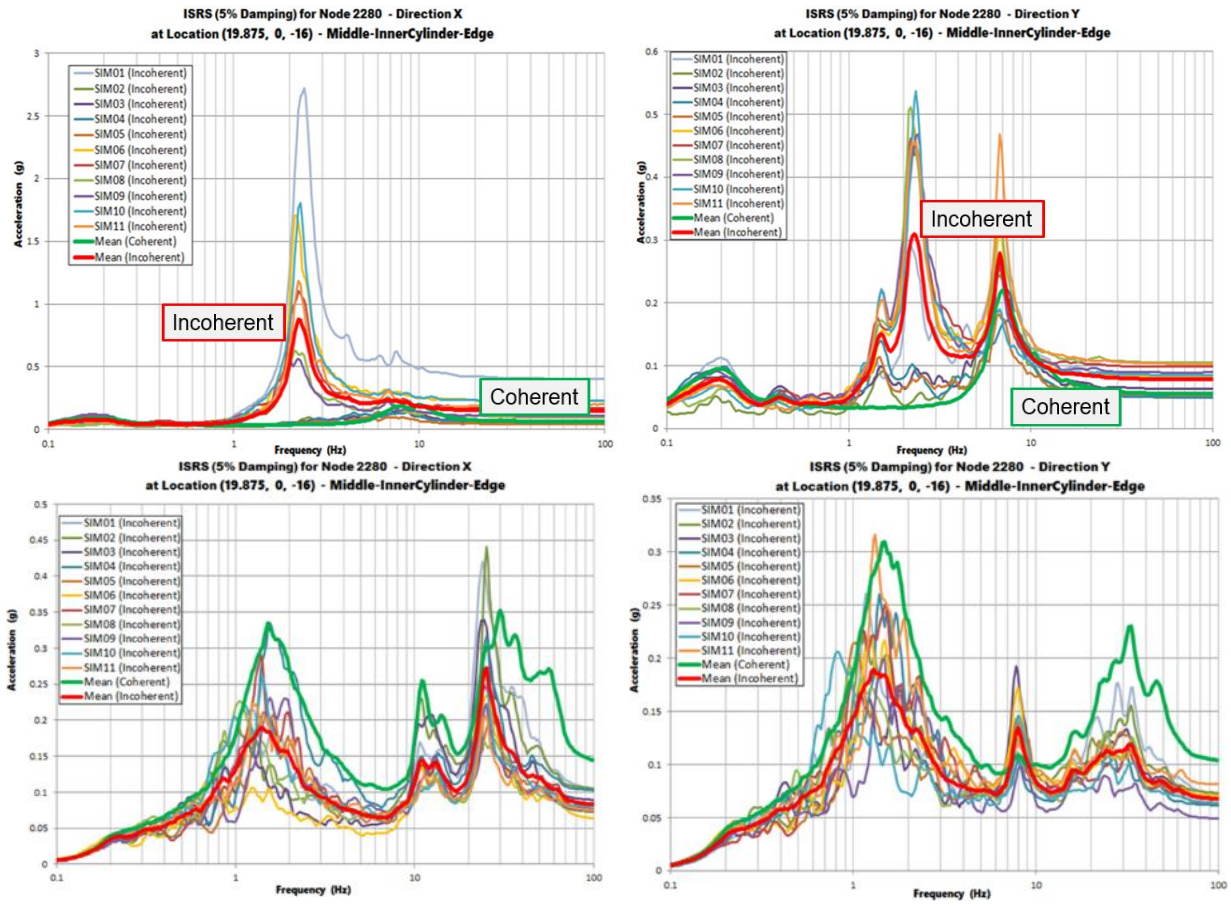

Figure 16 Mean ISRS at Elevation of -16 ft for Coherent (green) and Incoherent (red) Motions for Soil Site (upper plots) and Rock Site (lower plots); Incoherent Samples with Thin Lines

In contrast with the ISRS results for the soil site, the ISRS results for the rock site, show that the motion incoherency effects are favourable for almost all frequency ranges, with exception @ 9 Hz frequency peak which appears to be associated with a RV subsystem dynamic coupling with superstructure that is randomly excited by the differential support motions, this time in Y-direction for the hard-rock site. The reductions in the incoherent ISRS responses are larger in higher frequencies.

CONCLUDING REMARKS

The implemented seismic SSI methodology provides a reasonable and affordable design-basis seismic analysis for the base-isolated ARC-100 SMR design. Based on the SSI sensitivity study results, few additional SSI methodology adjustments are required to be considered in the following final design stages of the isolated structure.

It should be noted that for the computed ISRS, the effects of the isolator failures are critical for rock site under high-frequency inputs, while the effects of the seismic motion spatial variation (wave incoherency and wave passage) are critical for soil sites. Other SSI effects due to input variations such as the DBE spectrum component amplitude variations, FP isolation system stiffness variation, and mass eccentricity variations, even notable, appear to be less significant for the ARC-100 deeply embedded SMR structure response.

It was also shown that for the embedded ARC-100 SMR, the FP base-isolation system efficiency can be significantly enhanced creating a *hybrid* isolation system obtained by adding a local 3D BCS (spring-damper) isolation system placed at the RV beam supports. The local 3D BCS isolation system for the RV system *avoids the potential dynamic coupling* between the SMR superstructure and the RV system SSI responses, especially for the soil site.

REFERENCES

Abrahamson, N. (2007). Abrahamson, N. (2007). Effects of Spatial Incoherence on Seismic Ground Motions, *Electric Power Research Institute, Palo Alto, CA and US Department of Energy, Germantown, MD,* Report No. TR-1015110, December 2

ASCE 4-16 (2017) Seismic Analysis of Safety-Related Nuclear Structures, *ASCE/SEI*

ASCE 43-19 (2020) Seismic Design Criteria for Structures, Systems in Nuclear Facilities, *ASCE/SEI*

ASCE 7-22 (2022), Minimum Design Loads and Criteria for Buildings and Other Structures, *ASCE/SEI*

Fenz, D. M., and Constantinou, M. C. (2008b). "Mechanical Behavior of Multi-spherical Sliding Bearings." *MCEER-08-0007, State Univ. of New York*, Buffalo, NY.

Ghiocel, D.M. Lee, K., Lemley, D. Galunic, B. Odar, E. and Iotti, B. (2024). Study on Seismic SSI Effects for Deeply Embedded Base-Isolated SMR on Different Site Conditions. *SMIRT26 Conference, Division V,* Yokohama, Japan, March 3-8.

Ghiocel Predictive Technologies (2023) ACS SASSI NQA Version 4.3 An Advanced Computational Software for 3D Dynamic Analysis Including Soil-Structure Interaction, *GP Technologies, Inc., User Manuals, Revision 9,* Pittsford, New York

Nie J. (2019). Assessment Of Artificial Acceleration Time History Guidance in Standard Review Plan Section 3.7.1, "Seismic Design Parameters", *RIL 2019-01, Rev. 1, U.S. Nuclear Regulatory Commission.* Washington, DC